

ORIGINAL ARTICLE

Generation of prescriptions robust against geometric uncertainties in dose painting by numbers

EDMOND STERPIN, SARAH DIFFERDING, GUILLAUME JANSSENS, XAVIER GEETS, VINCENT GRÉGOIRE & JOHN A. LEE

Université catholique de Louvain, Center of Molecular Imaging, Radiotherapy and Oncology, Institut de Recherche Expérimentale et Clinique, Brussels, Belgium

ABSTRACT

Background. In the context of dose painting by numbers delivered with intensity-modulated radiotherapy, the robustness of dose distributions against geometric uncertainties can be ensured by robust optimization. As robust optimization is seldom available in treatment planning systems (TPS), we propose an alternative method that reaches the same goal by modifying the heterogeneous dose prescription (based on ^{18}F FDG-PET) and guarantees coverage in spite of systematic and random errors with known standard deviations Σ and σ , respectively.

Material and methods. The objective was that 95% of all voxels in the GTV_{PET} received at least 95% of the prescribed dose despite geometric errors. The prescription was modified by a geometric dilation of $\alpha\Sigma$ for systematic errors and a deconvolution by a Gaussian function of width σ for random errors. For a 90% confidence interval, $\alpha = 2.5$. Planning was performed on a TomoTherapy system, such that 95% of the voxels received at least 95% of the modified prescription and less than 5% of the voxels received more than 105% of the modified prescription. The applicability of the method was illustrated for two head-and-neck tumors.

Results. Systematic and random displacements larger than $\alpha\Sigma$ and σ degraded coverage. Down to 62.8% of the points received at least 95% of prescribed dose for the largest considered displacements (5 mm systematic translation and 3 mm standard deviation for random errors). When systematic and random displacements were smaller than $\alpha\Sigma$ and σ , no degradation of target coverage was observed.

Conclusions. The method led to treatment plans with target coverage robust against geometric uncertainties without the need to incorporate these in the optimizer of the TPS. The methodology was illustrated for head-and-neck cancer but can be potentially extended to all treatment sites.

In the last decade, voxel by voxel heterogeneous dose prescription, also known as dose painting by numbers (DPBN) [1], has gained interest in the radiotherapy community [1–6]. A heterogeneous dose prescription within the tumor volume in accordance with a given tumor phenotype, instead of uniform dose, is expected to improve the treatment outcome in terms of local control and/or side effects [1]. However, DPBN suffers from limitations that fall into three categories: 1) biological relevance and soundness of the heterogeneous prescription, based for instance on functional imaging like positron emission tomography (PET); 2) ability of the treatment delivery method to match the prescription with an actual

dose distribution; 3) geometric uncertainties in the broad sense (patient setup, tumor motion, etc).

At the moment, the first point has not been completely addressed and important questions are still raised in the literature [1–5]. As in Witte et al. [6], we assume that a prescription may be derived from PET images and needs to be delivered with minimal, controlled distortion.

Regarding the second issue, several groups have already established the technical feasibility of DPBN prescriptions for advanced treatments modalities (VMAT, TomoTherapy) using structure-based treatment planning systems [7,8]. In such systems, it is possible to closely approximate DPBN using a

Correspondence: E. Sterpin, Université catholique de Louvain, Center of Molecular Imaging, Radiotherapy and Oncology, Institut de Recherche Expérimentale et Clinique, Avenue Hippocrate 54, 1200 Brussels, Belgium. E-mail: esterpin@yahoo.fr.

(Received 16 October 2013; accepted 20 May 2014)

sufficient number of sub-contours within the volume of interest.

However, the literature is sparse regarding the inclusion of patient-related geometric errors. Usual margin recipes are valid for one or several uniform dose prescriptions [9], but not for DPBN.

In this study, we assume a non-uniform dose escalation in the tumor volume (the GTV). The objective is to find a methodology such that planned dose distributions are robust against geometric errors. In Witte et al. [6], geometric uncertainties are directly taken into account during the dose optimization process. This approach is termed ‘robust optimization’ and has been implemented by several groups for uniform prescriptions [10–13]. However, such robust optimization techniques are rarely available in commercial TPSs.

Illustrated with two head-and-neck cases, this study proposes a methodology that provides robust DPBN treatment plans, without specific optimization algorithms in the TPS. Our methodology has

therefore the potential to popularize robust DPBN. It accounts for geometric uncertainties by appropriately modifying the heterogeneous prescription. Although the chosen treatment modality is TomoTherapy, the methodology also applies to any other treatment modality relying on photon beams, provided that geometric errors do not exceed certain limits that are discussed further below and also that the treatment modality can accurately deliver heterogeneous prescriptions like those encountered in DPBN.

Material and methods

Consider a volume candidate to DPBN (the GTV) with a prescription $D_p(\mathbf{r})$ defined in all points \mathbf{r} of the CT geometry. The proposed workflow to deal with geometric uncertainties is illustrated in Figure 1 of Supplementary Appendix 1 ‘Mathematical formalism of the robust prescription’ (available online at <http://informahealthcare.com/doi/abs/10.3109/0284186X>.

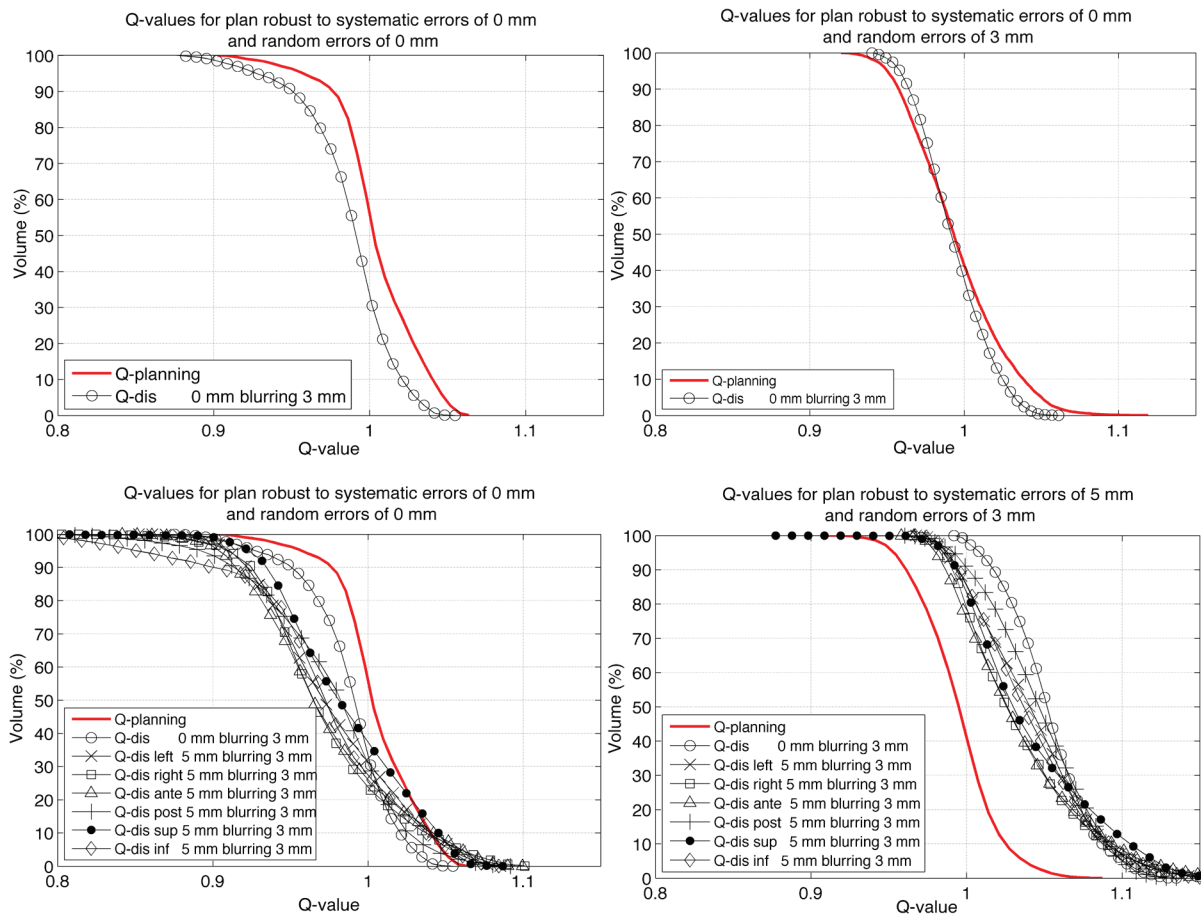


Figure 1. QVHs for patient 1 for shifted and blurred planned doses $D_{Planning}$ with respect to the original prescription D_p within GTV_{PET} . The robust prescriptions D_{RP} were computed with $(\alpha\Sigma, \sigma)$ mentioned in top of each figure. The legend of each figure details the systematic displacements (“dis”) that were simulated (no displacements, left, right, anterior, posterior, superior, inferior). Q-planning refers to QVH for $D_{Planning}$ with respect to D_{RP} within PTV_{PET} .

2014.930171). The method consists in calculating a modified prescription $D_{RP}(\mathbf{r})$, where RP stands for robust prescription, such that the planned dose distribution $D_{Planning}(\mathbf{r})$ is consistent with the original prescription $D_p(\mathbf{r})$ and robust against geometric errors, with regards to target coverage.

Quantification of treatment planning quality for non-uniform dose prescriptions

For the volume candidate to DPBN, treatment-planning quality is quantified using the decumulative quality-volume histogram (QVH) introduced by Vanderstraeten et al. [2], where the quality is defined in every voxel as the ratio of the planned dose to the prescribed dose.

For the TomoTherapy system, Deveau et al. [7] showed that the following quality criteria should be achievable using appropriate planning parameters: 1) more than 95% of the points receive at least 95% of the local prescription [$(V_{Q=0.95})_{Planning} \geq 95\%$]; 2) less than 5% of the points receive more than 105% of the local prescription [$(V_{Q=1.05})_{Planning} \leq 5\%$]; and 3) the mean quality value $(Q_{mean})_{Planning}$ is close to 1 within 1%. The subscript 'Planning' indicates that the metric quantifies the TPS ability to reproduce the prescription.

Robust prescription

Like in Witte et al. [6], a plan is considered to be robust when the planned dose is superior or equal to the prescribed dose in all points of the GTV within a certain tolerance (tumor coverage objective), in spite of geometric errors. Considering our planning objective [$(V_{Q=0.95})_{Planning} \geq 95\%$], this amounts to requiring that $(V_{Q=0.95})_{(\alpha\Sigma, \sigma)} \geq 95\%$, i.e. robustness against systematic shifts of $\pm\alpha\Sigma$ and random shifts with standard deviation σ (see [9] and Supplementary Appendix 1 available online at <http://informahealthcare.com/doi/abs/10.3109/0284186X.2014.930171>). As ensuring robustness of tumor coverage necessarily entails excess dose, the criterion $(V_{Q=1.05})_{(\alpha\Sigma, \sigma)} \leq 5\%$ no longer applies.

The methodology proposed in this study relies on the hypothesis of local shift invariance of the dose distributions, which is generally accepted for external photon therapy [9,14]. The presented methodology aims at satisfying $(V_{Q=0.95})_{(\alpha\Sigma, \sigma)} \geq (V_{Q=0.95})_{Planning} \geq 95\%$.

Robustness against systematic errors within a 90% confidence interval is ensured by dilating the original prescription $D_p(\mathbf{r})$ by an ellipsoid with vector radius $\alpha\Sigma$ ($\alpha = 2.5$). A PTV_{PET} is subsequently defined as the GTV_{PET} plus a margin of $\alpha\Sigma$. For the random errors, the dilated prescription is deconvolved with a

Gaussian function (zero mean and standard deviation σ), which corresponds to the assumed distribution of random errors. An exact solution to the deconvolution problem exists only if the prescription is the result of a convolution with a similar Gaussian function having a width greater or equal to σ . Due to various physical limitations, PET images may fulfill this requirement. In particular, their rather poor resolution is often approximately characterized with a Gaussian point-spread function.

Dilation is carried out prior to deconvolution. The order of these two operations is important to properly counteract the effect of random errors on the planned dose distributions (blurring does not have the same effect depending on whether the dose distributions reproduce original or dilated prescriptions). The effects of the aforementioned operations on the prescription are illustrated on a clinical case in Supplementary Appendix 2 (available online at <http://informahealthcare.com/doi/abs/10.3109/0284186X.2014.930171>) 'Illustrations of original, dilated and robust prescriptions on CT geometries' (available online at <http://informahealthcare.com/doi/abs/10.3109/0284186X>).

Preparation and execution of treatment planning tests

The proposed robust method was tested on two consecutive patients treated for locally advanced head-and-neck squamous cell carcinoma using a simultaneous integrated boost protocol (SIB). The prophylactic and the therapeutic PTVs were created from the CTV delineated on the planning CT according to published guidelines [15–17] and expanded by a 4 mm margin using a generic margin recipe [9]. For prophylactic and therapeutic PTVs, uniform doses of 56 and 70 Gy were prescribed, respectively.

The volume subject to DPBN (the GTV_{PET}) was automatically segmented on FDG-PET images with the gradient-based method previously implemented and validated by our group [18]. The subscript PET indicates that the external contour of the GTV_{PET} stems from the FDG-PET image. The FDG-PET images were acquired with a Philips Gemini PET-CT camera; the point-spread function was approximately Gaussian, with a FWHM of 7.5 mm, corresponding to a standard deviation of 3.2 mm. This gives the theoretical assurance that PET images from this camera may be deconvolved with a Gaussian function having a standard deviation up to 3.2 mm. Accurate dilation was guaranteed by resampling the PET images to 1 mm³ voxels with trilinear interpolation. Dilation itself used a nearest neighbor interpolator, leading to an accuracy of 0.5 mm. The validity of the present method does not depend on any particular segmentation method, provided the image may be deconvolved.

Consistently with Vanderstraeten et al. [2] and Witte et al. [6], the FDG uptake was converted linearly to a non-uniform dose-escalation from 70 (minimal uptake) to 86 Gy (maximal uptake).

Treatment planning was performed on a TomoTherapy TPS with a GPU architecture, whose accuracy is comparable to the extensively validated CPU algorithm [19–21]. Unless otherwise mentioned, the TPS parameterization of Deveau et al. [7] was followed (slice width of 1 cm; modulation factor of 3.0; and pitch of 0.43). The dose calculation grid was set in “fine” mode (about $2 \times 2 \times 2$ mm³ resolution).

Except for the boost volume (PTV_{PET}), the clinical constraints were $D_{95} \geq 95\%$ for target volumes, D_{mean} inferior to 30 and 26 Gy for ipsilateral and contralateral parotids, respectively, and D_2 inferior to 35 Gy for the spinal cord extended with a 5 mm margin.

The PTV_{PET} was divided into seven equally spaced sub-contours to approximate the DPBN prescription. For each volume enclosed in the i^{th} sub-contour (i going from 1 to 7), the minimum dose constraint equaled $70 + \frac{(i-1)}{7} [(D_{RP})_{\text{max}} - 70]$ Gy and the maximum $70 + \frac{i}{7} [(D_{RP})_{\text{max}} - 70]$. Another constraint was that D_{mean} between contours i and $i+1$ equaled the average of the minimum and maximum constraints. For the last contours, the maximum dose constraint equaled $(D_{RP})_{\text{max}}$.

Evaluation of the robustness of the non-uniform dose distributions to geometric displacements

Table I reports four couples of $(\alpha\Sigma, \sigma)$ values used to compute the robust prescriptions D_{RP} . For all cases, $\Sigma_x = \Sigma_y = \Sigma_z = \Sigma$ and $\sigma_x = \sigma_y = \sigma_z = \sigma$.

The robustness of the dose distributions was evaluated by: 1) shifting the dose distributions by a

Table I. Details of the systematic and random standard deviations values used for each patient included in this study.

Scenario #	T (mm)	σ_d (mm)	$(\alpha\Sigma, \sigma)$ used to determine
			robust prescription D_{RP} (mm)
1	2.5	1	(0,0)
			(2.5,1)
2	5	3	(0,0)
			(2.5,1)
			(5,3)
3	0	3	(0,0)
			(0,3)

The confidence interval for systematic errors was systematically 90% ($\alpha = 2.5$). The considered scenarios are detailed as well, with systematic displacements T and standard uncertainties α_d for random displacements.

displacement T in six directions (left, right, anterior, posterior, superior, and inferior); and 2) blurring the dose distributions with a Gaussian distribution with standard deviation σ_d . Subscript d was used to distinguish σ_d from σ used to compute the robust prescription. Symbols (T, σ_d) denoted the values of the displacements. Random ones were limited to σ_d lower or equal to 3 mm, thus lower than the resolution of the PET camera (3.2 mm standard deviation). Two sets of robustness tests were considered.

First, three scenarios evaluated tumor coverage for each patient. The associated values of (T, σ_d) are detailed in Table I. The three scenarios can be met in, respectively: 1) head-and-neck treatments using the best imaging tools available [22]; 2) thoracic treatments with baseline shift correction [23]; and 3) the idealized case of random errors only. To enhance readability of the results, only the scenarios involving displacements (T, σ_d) larger than or equal to $(\alpha\Sigma, \sigma)$ were considered.

In the second set of tests, the robustness was more finely tested for D_{RP} prepared with $(\alpha\Sigma, \sigma) = (2.5$ mm, 1 mm). Translations of 2.5, 3.12, 3.75, 4.37 and 5 mm were applied (which corresponds to values of Σ of 1, 1.25, 1.5, 1.75 and 2 mm, respectively). Random errors σ_d were kept at 1 mm. Ideally, the plan should be robust to displacements of maximum (2.5 mm, 1 mm).

Results

For the first set of tests, constraints on organs at risk were easily met for each pair $(\alpha\Sigma, \sigma)$ (see Table II). Figure 1 shows examples of QVHs for patient 1 for shifted and blurred D_{Planning} with respect to D_P within GTV_{PET} for the scenarios detailed in Table I. We focus on a possible crossing of the curves corresponding to each scenario and the one named Q_{planning} at $V_{Q=0.95}$, which is the threshold the robust prescription method aims at. When translations T exceed $\alpha\Sigma$, there is always at least one translation direction for which $(V_{Q=0.95})_{(T, \sigma_d)}$ is lower than the value of $(V_{Q=0.95})_{\text{Planning}}$ that was obtained to quantify treatment planning quality and listed in Table II. However, $(V_{Q=0.95})_{(T, \sigma_d)}$ is superior to the value of $(V_{Q=0.95})_{\text{Planning}}$ that was obtained to quantify treatment planning quality when translations T are smaller than $\alpha\Sigma$.

The only case where random errors do impact robustness of treatment planning by more than 1% [$(V_{Q=0.95})_{(T, \sigma_d)}$] is for a random error with 3 mm of standard deviation and no systematic error. In Figure 1a and b, target coverage is preserved when $\sigma = 3$ mm, whereas the QVH is shifted towards lower values when $\sigma = 0$ mm. Moreover, there is no significant excess dose to the GTV_{PET} observed if no systematic

Table II. Quantification of treatment planning quality using $(V_{Q=0.95})_{\text{Planning}}$ and $(V_{Q=1.05})_{\text{Planning}}$ computed within PTV_{PET} for D_{planning} with respect to D_{RP}

	$(\alpha\Sigma, \sigma)$ (mm)	$(V_{Q=0.95})_{\text{Plan}}$ (%)	$(V_{Q=1.05})_{\text{Plan}}$ (%)	$(Q_{\text{mean}})_{\text{Plan}}$	Ipsilateral Parotid D_{mean} (Gy)	Contralateral Parotid D_{mean} (Gy)	PRV Spinal cord D_2 (Gy)
		D_{Planned} vs. D_{RP} in PTV_{PET}					
Patient 1	(0,0)	96.3	3.8	1.005	24.7	24.6	28.5
	(0,3)	95.0	4.9	0.995	24.6	24.3	28.1
	(2.5,1)	99.9	2.8	1.006	24.4	24.3	27.6
	(5,3)	96.6	2.3	0.994	24.4	24.5	27.7
Patient 2	(0,0)	99.6	4.7	1.008	25.3	23.5	26.7
	(0,3)	98.0	4.5	1.000	24.2	24.4	27.0
	(2.5,1)	98.0	3.0	0.999	24.2	23.7	26.9
	(5,3)*	94.8	5.9	1.006	24.0	22.3	28.3

Robust prescriptions D_{RP} were computed for the listed couples of values $(\alpha\Sigma, \sigma)$. For all cases, $\Sigma_x = \Sigma_y = \Sigma_z = \Sigma$. Dose to the parotids and to the PRV of the spinal cord are also reported. *Pitch was reduced to 0.287 and modulation factor increased to 3.5.

translation occurs $(V_{Q=1.05})_{(T, \sigma_d)} [\leq 5\% \text{ in } \text{GTV}_{\text{PET}} \text{ for } (T, \sigma_d) = (0 \text{ mm}, 3 \text{ mm})]$.

As the margin was used for systematic errors, excess dose was inherently planned to the GTV_{PET} as soon as $\alpha\Sigma$ departed from zero. For $(\alpha\Sigma, \sigma)$ of (5 mm, 3 mm), $(V_{Q=1.05})_{(T, \sigma_d)}$ reached a maximum of 53%.

These observations are confirmed quantitatively for both patients in Table III.

Table IV reports the results of the second set of tests, where $(\alpha\Sigma, \sigma)$ is fixed to (2.5 mm, 1 mm). For systematic displacements larger than twice $\alpha\Sigma$, target coverage is clearly degraded, down to 94.5% and 92.2% for patients 1 and 2, respectively. However,

target coverage is preserved for translations up to 3.75 and 3.12 mm for patients 1 and 2, respectively.

Discussion

Overall, the results shown in Table II confirmed the ability of TomoTherapy to closely approximate voxel by voxel prescriptions, following similar guidelines as those proposed by Deveau et al. [7]. Despite our efforts during planning, we could not perfectly satisfy $(V_{Q=0.95})_{\text{Planning}} \geq 95\%$ and $(V_{Q=1.05})_{\text{Planning}} \leq 5\%$ for $(\alpha\Sigma, \sigma)$ of (5 mm, 3 mm) in patient 2. The likely cause is deconvolution, which sharpens the transition between dose levels and thus complicates the task of

Table III. Treatment planning robustness for various scenarios and robust prescriptions using $(V_{Q=0.95})_{(T, \sigma_d)}$ computed within GTV_{PET} for D_{planning} with respect to D_{P} .

	$(\alpha\Sigma, \sigma)$ (mm)	(T, σ_d) (mm)	$(V_{Q=0.95})_{(T, \sigma_d)} (D_{\text{planning}} \text{ vs. } D_{\text{P}} \text{ in } \text{GTV}_{\text{PET}}) (\%)$						
			Direction of translation						
			$T=0$	Left	Right	Anterior	Posterior	Superior	Inferior
Patient 1	(0,0)	(2.5,1)	96.1	94.5	95.1	93.8	93	99	93.8
	(2.5,1)	(2.5,1)	100	100	100	100	100	100	100
	(0,0)	(0,3)	90.4	N/A	N/A	N/A	N/A	N/A	N/A
	(0,3)	(0,3)	98.6	N/A	N/A	N/A	N/A	N/A	N/A
	(0,0)	(5,3)	90.4	68.3	66.0	64.8	72.9	76.9	73.5
	(2.5,1)	(5,3)	100	97.3	95.2	91.6	95.2	95.2	95.2
	(5,3)	(5,3)	100	100	100	100	100	100	100
Patient 2	(0,0)	(2.5,1)	99.4	98.3	98.9	94.7	96.1	99.6	98.7
	(2.5,1)	(2.5,1)	100	100	100	100	100	100	100
	(0,0)	(0,3)	98.3	N/A	N/A	N/A	N/A	N/A	N/A
	(0,3)	(0,3)	98.6	N/A	N/A	N/A	N/A	N/A	N/A
	(0,0)	(5,3)	98.3	80.1	74.5	69.3	78.0	84	78.8
	(2.5,1)	(5,3)	100	94.5	92.2	92.2	94.3	98	96.3
	(5,3)	(5,3)	100	100	100	100	100	100	100

All D_{planned} distributions were blurred by a Gaussian function with standard deviation σ_d . Translations (T) were also applied to the patient geometry in the six directions. The case of no systematic shift was considered as well ($T=0$). For all cases, $\Sigma_x = \Sigma_y = \Sigma_z = \Sigma$. Values are in bold type when $(V_{Q=0.95})_{(T, \sigma_d)} \geq (V_{Q=0.95})_{\text{Planning}}$ is not satisfied. When $(V_{Q=0.95})_{(T, \sigma_d)} \geq 95\%$ is not satisfied either, values are in bold and italic type. N/A stands for not applicable because there are no translations to be simulated.

Table IV. Quantification of treatment planning robustness for a specific robust prescription using $(V_{Q=0.95})_{(T, \sigma_d)}$ computed within GTV_{PET} for $D_{Planning}$ with respect to D_P .

(T, σ_d) (mm)	Minimum $(V_{Q=0.95})_{(T, \sigma_d)}(D_{Planning})$ vs. D_P in GTV_{PET} (%)	
	Patient 1 $(V_{Q=0.95})_{Planning} = 99.9\%$	Patient 2 $(V_{Q=0.95})_{Planning} = 98\%$
(2.5,1)	100	100
(3.12,1)	100	99.5
(3.75,1)	99.9	97.9
(4.37,1)	98.9	95.5
(5,1)	94.5	92.5

For both patients, $D_{Planning}$ was optimized from a robust prescription with $(\alpha\Sigma, \sigma) = (2.5 \text{ mm}, 1 \text{ mm})$. All $D_{Planning}$ distributions were blurred by a Gaussian function with standard deviation σ_d . Translations (T) were also applied to the patient geometry in the six directions. The minimal value of $(V_{Q=0.95})_{(T, \sigma_d)}$ is reported. For all cases, $\Sigma_x = \Sigma_y = \Sigma_z = \Sigma$. Values are in bold type when $(V_{Q=0.95})_{(T, \sigma_d)} \geq (V_{Q=0.95})_{Planning}$ is not satisfied. When $(V_{Q=0.95})_{(T, \sigma_d)} \geq 95\%$ is not satisfied as well, values are in bold and italic type.

the TPS to match the prescription (limitation by the finite penumbra [24]). The deconvolution process increases the dose gradient and thus the difficulty in matching the prescription.

Results shown in Figure 1 and Table III demonstrate that the objective of robustness is achieved for values of T and σ_d both lower than or equaling $\alpha\Sigma$ and σ . The effect of random errors is far less important than that of systematic errors. Only the case of (T, σ_d) of (0 mm, 3 mm) applied to plans computed with $(\alpha\Sigma, \sigma) = (0 \text{ mm}, 0 \text{ mm})$ degraded target coverage (Table III) beyond 1%. However, the methodology proved to enhance target coverage when accounting for random errors implicitly in the prescription. No degradation was observed for $(V_{Q=0.95})_{(T, \sigma_d)}$ for (T, σ_d) of (0 mm, 3 mm) applied to plans set up with $(\alpha\Sigma, \sigma) = (0 \text{ mm}, 3 \text{ mm})$ for both patients. When considering only random errors, no excess dose was observed either, as shown in Figure 1b. This was expected since only the shape of the prescription is modified during the convolution. Moreover, the deconvolution process has the advantage that it does not require an a priori knowledge of the dose distribution (compared to the margin added for random errors in the case of homogeneous dose distributions, which assume spherical symmetry, perfect conformation and Gaussian penumbra [9]). Notice, however, that the deconvolution is an ill-posed problem and the exact solution of the deconvolution problem might not exist. This would occur if σ were larger than the resolution of the PET images. As the correspondence between prescription (robust or not) and planning quality does not need to be strict, an approximate solution to

deconvolution might still lead to dose distributions that satisfy $(V_{Q=0.95})_{(T, \sigma_d)} \geq (V_{Q=0.95})_{Planning} \geq 95\%$ without any unnecessary excess dose. This is performed in algorithms implementing robust optimization, which actually do attempt to solve implicitly a deconvolution problem using an iterative approach but during the dose optimization process. The validity of the present method for prescriptions and values of σ larger than the resolution of the PET images requires further investigation. In this case, another approach might be necessary that still circumvents robust optimization of the *planned* dose. This approach could actually involve robust optimization of the *prescription*, with a model accounting for random errors. The objectives of the optimization process would then be: 1) coverage of the (dilated) prescription; and 2) minimization of the excess dose to the GTV_{PET} .

To reach robustness in spite of systematic errors, some excess dose must be delivered but should be kept as low as possible. Considering the isotropic expansion used for the clinical examples, the dose in the dilated prescription at every point equals the maximum dose in the original prescription within a sphere of radius $\alpha\Sigma$ around the considered point. Assuming that the TPS can match with comparable accuracy the original and dilated prescriptions, this process necessarily ensures that target coverage for systematic displacements of $T = \alpha\Sigma$ will be better than or equal to target coverage achieved during treatment planning (provided that the dose distributions are shift-invariant). This approach is conservative. For instance, points that are not displaced towards the edge of the dilated boost volume (the PTV_{PET}) but rather towards a hot spot get moved to higher dose regions on average. This phenomenon combined to the fact that the planned dose is not perfectly conformal [$(V_{Q=1.05})_{Planning}$ equals 2.8 and 3.0 % for patients 1 and 2, respectively] may explain the good coverage obtained for values of T slightly exceeding $\alpha\Sigma$ (Table IV). For both patients, coverage starts to degrade from 3.75Σ , thus a confidence interval of more than 99%.

A dilation of $\alpha\Sigma$ is also extremely conservative if we consider a dose tolerance of, i.e. 5% at every point. In such case, the dilation of $\alpha\Sigma$ could be reduced by the distance between any point in the heterogeneous prescription and the closest point that has a 5% lower prescription. This would allow for a flexible margin from zero to $\alpha\Sigma$, depending on the local gradient in the prescription (a large gradient leads to a larger margin). However, such strategy potentially violates the condition $(V_{Q=0.95})_{(\alpha\Sigma, \sigma)} \geq (V_{Q=0.95})_{Planning}$ and was not considered in the present study.

To further evaluate the efficiency of the robust prescription method to avoid unnecessary excess dose, let us compare our results to a robust optimization option as implemented by Witte et al. [6], who use robust optimization. For $(\alpha\Sigma, \sigma) = (5 \text{ mm}, 3 \text{ mm})$, $(V_{Q=1.05})_{(T, \sigma_d)}$ may reach 53%. The prescription range for the head-and-neck case in Witte et al. (70–85 Gy) is similar to the one used here, allowing for a fair comparison, at least to some extent (the acceptability criterion of Witte et al. is different since 99% of the points must receive more than 95% of the dose). At $(V_{Q=1.05})_{(T, \sigma_d)}$ the excess dose in absolute values is within 3.5–4.3 Gy (5% of prescribed dose ranging from 70 to 86 Gy). This conversion to absolute dose values is necessary to compare with Witte et al. who use ΔVH to assess treatment planning quality. Using a 90% confidence interval and hence assuming $(\alpha\Sigma, \sigma) = (6.25 \text{ mm}, 2.5 \text{ mm})$, Witte et al. report an excess dose of 4 Gy within, roughly, 30 up to almost 70% of the GTV, thus comparable to the 53% achieved in the present study.

As one of its main advantages, robust optimization can potentially take into account modifications of the dose distributions caused by geometric errors. The hypothesis of shift invariance of the dose distributions is common in the computation of safety margins for homogeneous distributions. Witte et al. [6] also rely on this hypothesis to implement robust optimization. Nevertheless, significant modifications of the dose distributions because of geometrical shifts of the patient have been reported [25]. Dose distributions sensitive to patient shifts should therefore be recomputed during robust optimization to comprehensively address the problem of geometric uncertainties in DPBN, especially for large geometric errors.

At the present time, a formal validation of our methodology requires more patient cases as well as other target locations than head-and-neck. This study aimed to demonstrate that, under some reasonable hypotheses, robust DPBN treatments can be planned without robust optimization techniques. The proposed method yields satisfactory results in terms of target coverage and limited excess dose to the GTV_{PET}. It proceeds by modifying the dose prescription, using first dilation to compensate for systematic errors and then deconvolution for random errors. The latter operation remains formally valid for random errors smaller than the resolution of the PET images. Random deviations of about 1 mm did not show any significant impact based on the considered cases. In contrast, systematic errors have a much stronger impact but they can be taken into account quite easily without robust optimization. Future investigations aim at applying our approach to other target locations than head-and-neck and also to larger random errors.

Acknowledgements

The medical and physics teams of the radiotherapy department of Cliniques Universitaires Saint-Luc are acknowledged for their precious help. Sarah Differding is a PhD student supported by a grant Télévie from the Belgian ‘Fonds National pour la Recherche Scientifique’ (Grant Télévie-FC 92318-n°7460113F)”. J. A. Lee is a Research Associate of the Belgian ‘Fonds National pour la Recherche Scientifique’ (Research Associate-FC 63880)”.

Declaration of interest: The authors report no conflicts of interest. The authors alone are responsible for the content and writing of the paper.

References

- [1] Bentzen SM. Theragnostic imaging for radiation oncology: Dose-painting by numbers. *Lancet Oncol* 2005;6:112–7.
- [2] Vanderstraeten B, Duthoy W, De Gersem W, De Neve W, Thierens H. [18F]fluoro-deoxy-glucose positron emission tomography ([18F]FDG-PET) voxel intensity-based intensity-modulated radiation therapy (IMRT) for head-and-neck cancer. *Radiother Oncol* 2006;79:249–58.
- [3] Christian N, Lee JA, Bol A, De Bast M, Jordan B, Grégoire V. The limitation of PET imaging for biological adaptive-IMRT assessed in animal models. *Radiother Oncol* 2009;91:101–6.
- [4] Tanderup K, Olsen DR, Grau C. Dose painting: Art or science? *Radiother Oncol* 2006;79:245–8.
- [5] Aerts HJWL, Lambin P, Ruyscher DD. FDG for dose painting: A rational choice. *Radiother Oncol* 2010;97:163–4.
- [6] Witte M, Shakirin G, Houweling A, Peulen H, van Herk M. Dealing with geometric uncertainties in dose painting by numbers: Introducing the ΔVH . *Radiother Oncol* 2011; 100:402–6.
- [7] Deveau MA, Bowen SR, Westerly DC, Jeraj R. Feasibility and sensitivity study of helical tomotherapy for dose painting plans. *Acta Oncol* 2010;49:991–6.
- [8] Korreman SS, Ulrich S, Bowen S, Deveau M, Bentzen SM, Jeraj R. Feasibility of dose painting using volumetric modulated arc optimization and delivery. *Acta Oncol* 2010;49: 964–71.
- [9] van Herk M, Remeijer P, Rasch C, Lebesque JV. The probability of correct target dosage: Dose-population histograms for deriving treatment margins in radiotherapy. *Int J Radiat Oncol Biol Phys* 2000;47:1121–35.
- [10] Unkelbach J, Oelfke U. Inclusion of organ movements in IMRT treatment planning via inverse planning based on probability distributions. *Phys Med Biol* 2004;49:4005–29.
- [11] McShan DL, Kessler ML, Vineberg K, Fraass BA. Inverse plan optimization accounting for random geometric uncertainties with a multiple instance geometry approximation (MIGA). *Med Phys* 2006;33:1510–21.
- [12] Witte MG, van der Geer J, Schneider C, Lebesque JV, Alber M, van Herk M. IMRT optimization including random and systematic geometric errors based on the expectation of TCP and NTCP. *Med Phys* 2007;34:3544–55.
- [13] Gordon JJ, Sayah N, Weiss E, Siebers JV. Coverage optimized planning: Probabilistic treatment planning based on dose coverage histogram criteria. *Med Phys* 2010;37:550–63.
- [14] Mexner V, Wolthaus JWH, van Herk M, Damen EMF, Sonke J-J. Effects of respiration-induced density variations

- on dose distributions in radiotherapy of lung cancer. *Int J Radiat Oncol Biol Phys* 2009;74:1266–75.
- [15] Grégoire V, Coche E, Cosnard G, Hamoir M, Reyckler H. Selection and delineation of lymph node target volumes in head and neck conformal radiotherapy. Proposal for standardizing terminology and procedure based on the surgical experience. *Radiother Oncol* 2000;56:135–50.
- [16] Grégoire V, Levendag P, Ang KK, Bernier J, Braaksma M, Budach V, et al. CT-based delineation of lymph node levels and related CTVs in the node-negative neck: DAHANCA, EORTC, GORTEC, NCIC, RTOG consensus guidelines. *Radiother Oncol* 2003;69:227–36.
- [17] Grégoire V, Eisbruch A, Hamoir M, Levendag P. Proposal for the delineation of the nodal CTV in the node-positive and the post-operative neck. *Radiother Oncol* 2006;79:15–20.
- [18] Geets X, Lee J a, Bol A, Lonneux M, Grégoire V. A gradient-based method for segmenting FDG-PET images: Methodology and validation. *Eur J Nucl Med* 2007;34:1427–38.
- [19] Chen Q, Lu W, Chen Y, Chen M, Henderson D, Sterpin E. Validation of GPU based TomoTherapy dose calculation engine. *Med Phys* 2012;39:1877–86.
- [20] Sterpin E, Salvat F, Olivera GH, Vynckier S. Monte Carlo evaluation of the convolution/superposition algorithm of Hi-ArtTM Tomotherapy in heterogeneous phantoms and clinical cases. *Med Phys* 2009;36:1566–75
- [21] Sterpin E, Tomsej M, Cravens B, Salvat F, Ruchala K, Olivera GH, et al. Monte Carlo simulation of the Tomotherapy treatment unit in the static mode using MC HAMMER, a Monte Carlo tool dedicated to Tomotherapy. *J Phys: Confer Ser* 2007;74:021019.
- [22] Boswell S, Tomé W, Jeraj R, Jaradat H, Mackie TR. Automatic registration of megavoltage to kilovoltage CT images in helical tomotherapy: An evaluation of the setup verification process for the special case of a rigid head phantom. *Med Phys* 2006;33:4395–404.
- [23] Wolthaus JWH, Sonke J-J, van Herk M, Belderbos JS, Rossi MMG, Lebesque JV, et al. Comparison of different strategies to use four-dimensional computed tomography in treatment planning for lung cancer patients. *Int J Radiat Oncol Biol Phys* 2008;70:1229–38.
- [24] Sterpin E, Chen Y, Lu W, Mackie TR, Olivera GH, Vynckier S. On the relationships between electron spot size, focal spot size, and virtual source position in Monte Carlo simulations. *Med Phys* 2011;38:1579–86.
- [25] McShan DL, Kessler ML, Vineberg K, Fraass B. Inverse plan optimization accounting for random geometric uncertainties with a multiple instance geometry approximation (MIGA). *Med Phys* 2006;33:1510–21.

Supplementary material available online

Supplementary Appendix 1–2 and Figures 1 and 2.